The Impact of Systematic Extraction and Data Handling Errors on the Photometric Quality of High Dispersion LWP Data

C.A. Grady, M.A. Smith, M.P. Garhart, and G.F. Fireman
February 15, 1989

ABSTRACT

We present a summary of recent analysis of LWP high dispersion spectra as part of the on-going program to develop a better ripple correction for that camera. Systematic misregistration of the spectral orders, especially at the short-wavelength ends of each order, together with the introduction of spurious features into the net spectrum, compromise the quality of the net spectra, and have, to date, precluded derivation of a reliable echelle ripple correction for the LWP.

1. Introduction

A distinguishing characteristic of echelle spectra is the large variation in sensitivity as a function of wavelength within each spectral order. When the net spectra in successive orders are plotted as a function of wavelength, a scalloped, or "ripple" pattern results, and must be corrected prior to absolute calibration, or measurement of all but the narrowest spectral features. The ripple correction in use for the LWP (Ake 1985) has long been known to poorly fit the observed spectra at the ends of the orders, particularly for spectra which are not low background, continuum sources. Residuals as large as 10-20% are common, resulting in difficulties in line profile fitting, in continuum normalization, and in comparing high dispersion data with low dispersion observations. The Three Agencies, therefore, identified improvement of the LWP ripple correction, especially for data processed with the new LWP Intensity Transfer Function (ITF), as a high priority calibration project, that is not only important in its own right, but essential to the success of the high dispersion absolute calibration.

1.1 Fitting Techniques

Ake (1982) found that the wavelength dependence of the variation in sensitivity within an IUE high dispersion order could be fit by

$$R(\lambda) = sinc^2\left(\frac{\pi m\alpha \mid \lambda - K/m \mid}{\lambda}\right) \qquad (1)$$

where m is the spectral order number, K is a parameterized form of the echelle grating constant, α is an adjustable parameter which physically corresponds to the width of the blaze pattern, and sinc(x)=sin(x)/x. Two techniques for determining the free parameters K and α have been used in the calibration of the IUE echelle modes. The first approach is to fit the entire observed spectrum to equation (1) in a least squares sense. This approach, termed fitting the $sinc^2$ function has the advantage of using all of the data, including the spectral data at the camera sensitivity maximum. It is sensitive to the presence of uncorrected blemishes, cosmic ray hits, and spectral lines. An alternate approach, developed by Barker (1984), adjusts the free parameters to minimize the differences between the ripple-corrected net fluxes in the region of wavelength overlap between successive orders. As noted by Grady and Garhart (1989), this technique is not sensitive to the presence of spectral lines, but is very sensitive to the presence of noise, which would not be expected to be correlated in two successive orders.

1.2 Using the Barker Technique

Based on success in applying the Barker technique to the SWP (Grady and Garhart 1989), we began our analysis of the LWP echelle blaze function using this technique. Since the calibration configuration to be used in the bulk reprocessing had not yet been defined, and only a limited number of calibration spectra had been processed with the new LWP ITF (ITF2), our initial analysis was confined to LWP data processed with the "old" ITF (ITF1), we wished to explore whether increasing the number of spectra included in the analysis, over those available to Ake in 1985, would improve the correction. Our analysis was restricted to orders 80-100, to ensure adequate order overlap, and sufficient signal that noise in the data would not dominate the least squares fitting.

At first inspection, the results of the Barker technique appeared promising. The K parameter (which is proportional to the central wavelength in each order) showed a weak and linear dependence on order number for orders 80-100, slower than that found by Ake (1985). The spectral width parameter α was held fixed for this analysis at the default value of 0.895 which had been found by Ake (1985). Unfortunately, inspection of spectral data which had been ripple corrected using the data derived from the Barker technique revealed residuals as large as for the default Ake (1985) correction (typically 3-12% for optimally exposed continuum source spectra).

1.2 Explicitly Fitting the Sinc^2 Function

With this disheartening result, we next explored the possibility that the spectral width might depend upon order number. This could physically arise if the camera's flat field response to spectral (non-monochromatic) light was different from its response to the UV flood. For this analysis we produced software to least squares fit the entire observed net spectrum to the theoretical sinc^2 function predicted for an echelle grating (see Grady and Garhart 1989 for the equation). Only preliminary testing on a few spectra was done. We found, again, a slow and linear dependence of K on order number for orders 80-100, but dramatic variation in the spectral width parameter α (≥ 0.15) from order to order. Inspection of successive orders on the photowrites suggested that this dependence might not be physical. The acid test came with inspection of spectral data which were "ripple-corrected" using this latest set of parameters. We found, much to our dismay, that residuals of at least 20% were present in the low orders, which were optimally exposed. By order 100 the residuals were as large as 50%, which was clearly unacceptable. A preliminary analysis by Ponz and Cassatella (1985, private communication) of 7 early LWP high dispersion spectra produced similar ripple coefficients, indicating that the difficulty was likely to arise from a deficiency in the model for the ripple function, rather than an artifact of the software or ITF used in the analysis.

2. Inspection of the MEHI file records

The results of the two fitting approaches suggested that the net spectra showed sensitivity variations with wavelength other than those predicted by echelle grating theory. In order to test this hypothesis, we began a program of inspecting selected orders of MEHI files. The bulk of our analysis was confined to two spectra, LWP 7198 and LWP 7913, both of η UMa, which had been reprocessed using the new LWP ITF, and the old version of TCCAL, since this combination of calibrations has been selected for the bulk reprocessing to begin in late 1989. Inspection of other processed versions of these two spectra (new ITF, new TCCAL, and old ITF, old TCCAL) as well as spot checks of some additional spectra suggests that while the point to point FN vary with choice of calibration, the overall trends seen in the data are independent of choice of calibration data.

Two problems were identified. The first involves the flux levels in the gross and interorder background spectra. The second problem is introduced into the net spectrum by the choice of filters used to smooth the background before generating the net spectrum.

3. Flux Asymmetries in the Gross and Interorder Backgrounds

Figure 1 shows the IUESIPS-generated gross, smoothed interorder, and net spectra for LWP 7913 in order 100. The short wavelength end of the gross spectrum, which is smoother than the long wavelength end apparently due to camera defocussing, is lower in FN. Similarly the interorder background is higher at short wavelengths than at long wavelengths. The asymmetry is even more exaggerated in the net spectrum. Figure 2 shows an interactive, single-pixel wide extraction of the gross spectrum for order 100 from a byte-scaled version of the photometrically corrected image. No significant asymmetry is present. Figure 3 shows the interorder tracings on either side of the order which are averaged to form the interorder background. These tracings have essentially a constant mean level, although the noise amplitude changes, as expected from the camera characteristics.

The observed asymmetry in the extracted gross spectrum, together with the presence of excess interorder background flux, not seen in the photometrically-corrected image suggested that the high dispersion orders might be systematically mis-registered on the short-wavelength side of the LWP echelle format. We confirmed this suggestion by comparing the predicted order centroids, as calculated in the IUESIPS image processing, with the actual order centroids in a 4X over-exposed η UMa spectrum. The deeply exposed image was chosen so that adequate signal levels would be present at the ends of the orders in the low-sensitivity, short-wavelength portion of the camera. We found that the registration was good, to within a pixel of the actual centroids, in the center and long-wavelength portion of all the orders, but was systematically offset as much as 1.5-2 pixels above the actual centroid location at the short-wavelength side of the orders (Figure 3). The offsets was particularly pronounced in the higher orders, where camera sensitivity is low. A numerical experiment with a single-pixel wide slit having the length of the IUESIPS slit suggested that mis-registration of this amount would account for a 10-20% decrease in flux levels in the extracted gross spectrum, which is in agreement with the observed flux deficit.

The source of the mis-registration is currently under investigation. The spectral registration is sensitive both to the dispersion relation and to the geometric distortion correction. Further corrections for thermally-induced displacements of the high dispersion spectral format can affect data, but were not a factor in our test data which were obtained at the reference THDA for the LWP. We note that the portion of the LWP camera affected by the mis-registration has both the largest geometric distortion, and is relatively devoid of emission lines currently used to derive the dispersion relation.

4. Introduction of Features into the Net Spectrum

The net spectrum shown in Figure 1 contains two pronounced "absorption" features not present in the gross spectrum. These features coincide in wavelength with two broad "emission" features in the interorder background occuring at approximately the position of the change from small noise amplitude to large noise amplitude near 2310 Å. Inspection of the photometrically corrected image for this spectrum (Figure 4) confirms the increased pixel-to-pixel structure in the interorder and gross spectra, so the noise characteristics appear to be an intrinsic feature of the data, not an artifact of subsequent image processing. Numerical experiments with the unsmoothed interorder background provided in the MEHI file indicate that these ""emission" features are the result of the choice of median and mean filters for smoothing the background. Similar behavior is seen in other orders, although the fact that the interorder background in the high LWP orders is a significant fraction of the amplitude of the gross spectrum, causes features in the smoothed background to have a significant impact on the net spectrum. Spurious spectral features are introduced into the lower orders, but are less immediately visible due to the greater camera sensitivity at those wavelengths.

5. Alternate Techniques for Generating a Smooth Background

The original justification for smoothing the interorder background was to avoid introducing spectral features or cosmic ray hits into the net spectrum. The median filter is intended to remove the effects of any normal incidence cosmic ray hits from the background prior to smoothing the data by the mean filters. Use of this filter also assumes that any spikes in the interorder spectrum are not intrinsic to the camera. The spectral features, particularly in the high orders of the SWP, are due to light from adjacent spectral orders providing a non-zero signal at the positions of interorder extraction on either side of the spectral order of interest. The mean (boxcar) filters used in IUESIPS are intended to smooth over any such features so that only a smooth, approximately constant background level is subtracted. An implicit assumption of this approach is that the noise characteristics of the interorder background are uniform across an order, and do not dominate the interorder signal. This assumption, while true for the SWP, is not satisfied for the LWP.

We have tried a number of combinations of median and mean filters on order 100 of LWP 7913. We find that only mean filters with widths greater than 100 pixels appreciably reduce the amplitude of the high frequency bumps noted in Figure 1. Since the mean filter is a convolution with the original data, the price of this reduction is an overall elevation of the background level in some parts of the order not as severely affected in the original IUESIPS processed version. Overall, the combination of median and mean filters does not appear to effectively handle the noise characteristics of LWP interorder data.

As an alternate approach, we explored fitting the observed interorder spectrum by a simple, smooth function. Due to the curvature of the interorder backgrounds available on the MEHI tape, we selected a quadratic polynomial as the fitting function. Based on the flat interorder tracings observed in the photometrically corrected image, we feel that this kind of polynomial is non-physical, but can illustrate the feasiblity of fitting the background, rather than simply filtering it. Prior to fitting, we divided the interorder spectrum into 2 Å bins. For each bin we computed the mean FN level, and then least squares fit the binned data to a second order polynomial. Our brief inspection of the PI image suggested that, if the extraction were handled better, a linear or constant model might be more appropriate. The result of this fitting is a highly smoothed background which results in much reduced distortion of the net spectrum (Figure 5a,b) Figure 6 shows the resulting net spectrum, which is no longer contaminated by the spurious "spectral lines" so evident in the MEHI version of the net spectrum.

6. Conclusions

We have identified two potential problems with the handling of the LWP gross and interorder background spectra which, when combined, appear to account for the large amplitude distortions of the net spectrum from the sinc^2 dependence predicted by echelle grating theory. Mis-registration of the spectral orders at the short wavelength end of each order results in loss of light from the gross spectrum, an interorder background which contains the source spectrum, and a net spectrum with sensitivity maximum which is skewed from the true response of the grating and camera. Filtering of the interorder background by the currently implemented median and mean filters results in the introduction of broad spectral features which can mimic source features, particularly in high $v \sin i$ or gravity continuum sources. A further effect of this contamination of the net spectrum is to cause apparent variations in spectral width which are not physical.

We are continuing the analysis of both of these problems in the hope of identifying the source of the mis-registration, and to obtain an improved algorithm for handling the interorder background.

References

Ake, T.B. 1985, *Record of the IUE NASA/ESA/SERC Three Agency Coordination Meeting, November 13-16 1984 at GSFC*, A-138.

Barker, P.K. 1984, *A. J.,* **89**, 899.

Grady, C.A., and Garhart, M.P. 1989, *IUE NASA Newsletter*, **37**, (in press).

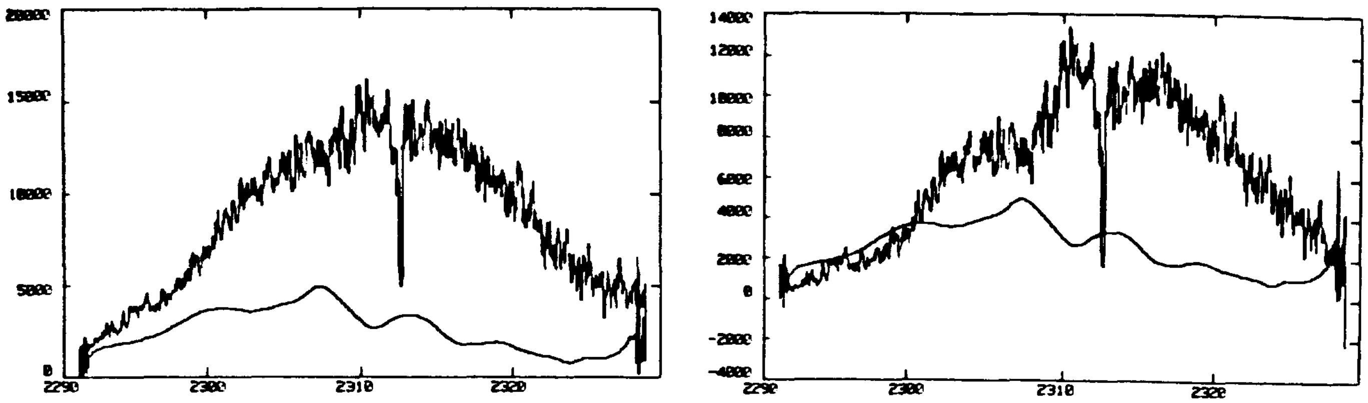

Figure 1 (left): Gross and smoothed interorder background for order 100 of LWP 7913 (η UMa), as processed by IUESIPS with the new LWP ITF and old TCCAL. (right): Net spectrum and smoothed interorder background for the same order and image. Distortions are introduced into the net spectrum as a result of smoothing across the change in noise amplitude in the unsmoothed background.

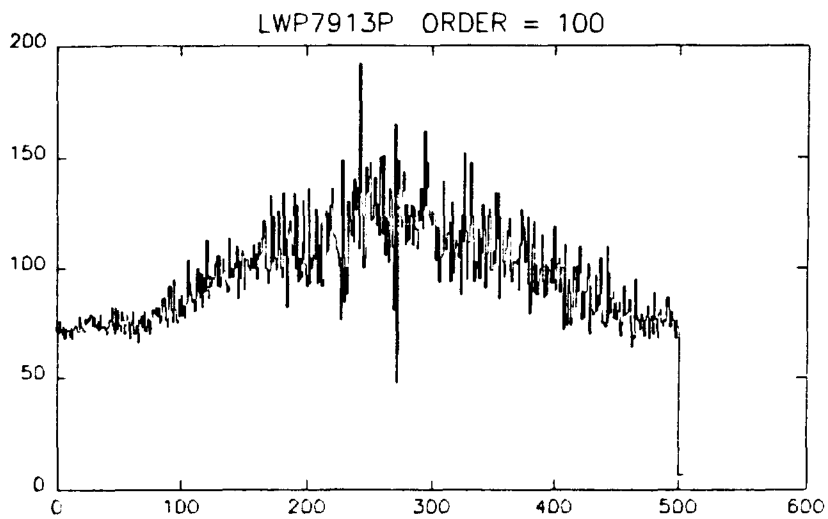

Figure 2: Gross spectrum for order 100 of LWP 7913 interactively extracted from a byte-scaled version of the photometrically-corrected image. The extraction slit is a single pixel wide, accounting for the larger noise amplitude compared to the IUESIPS extraction shown in Figure 1. The short wavelength (small sample number) end of the order is not depressed compared to the long wavelength end. Such a depression is characteristic of the IUESIPS extraction.

Figure 3: Overlay of the centroid of the IUESIPS extraction slit on a 4X overexposed spectrum of η UMa. A small portion of the image near order 100 is shown including the short wavelength side of the order. The extraction slit is misregistered with respect to the actual data by as much as 1.5-2 pixels, resulting in the asymmetry in the IUESIPS extracted gross spectrum of the kind shown in Figure 1.

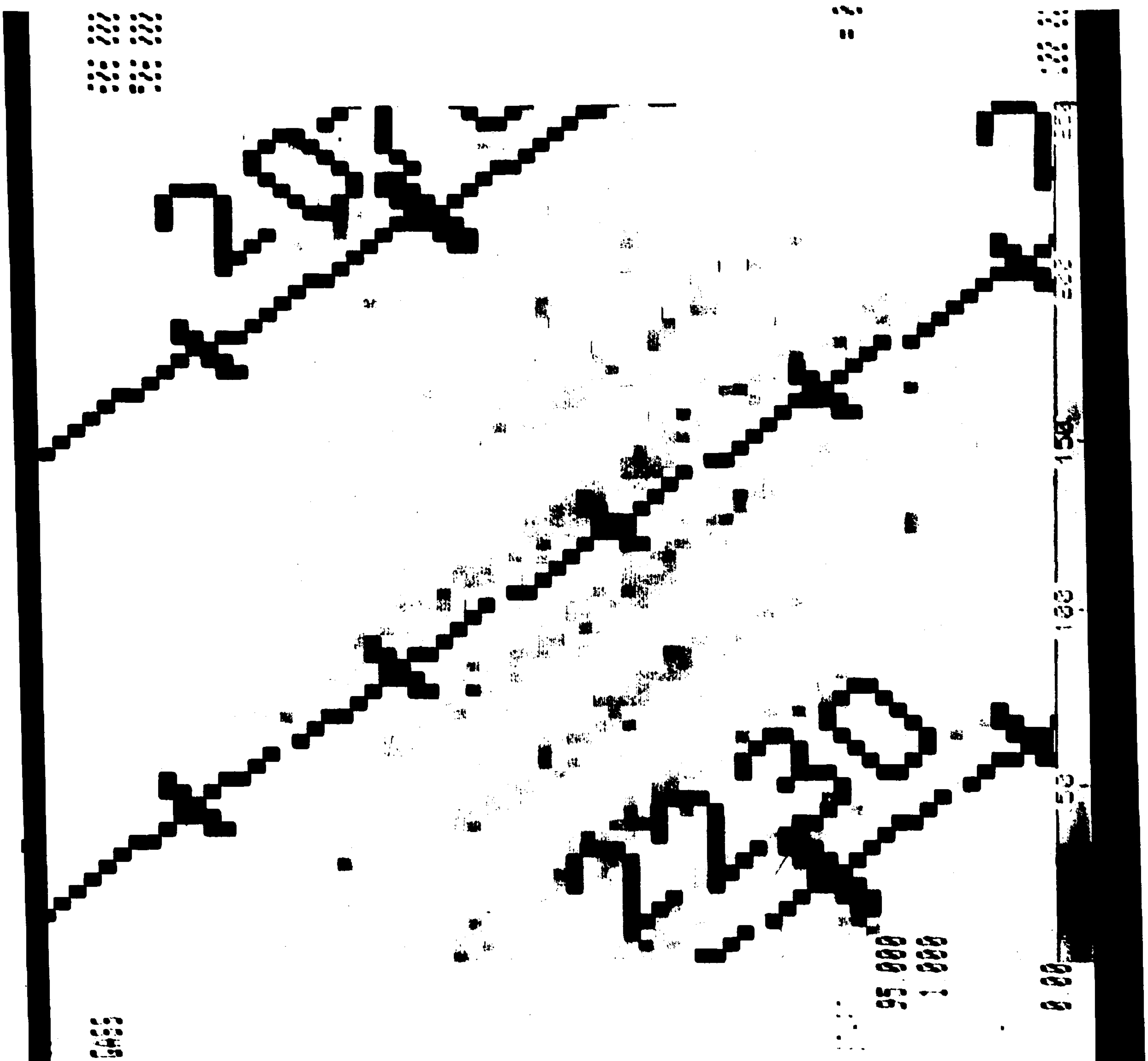

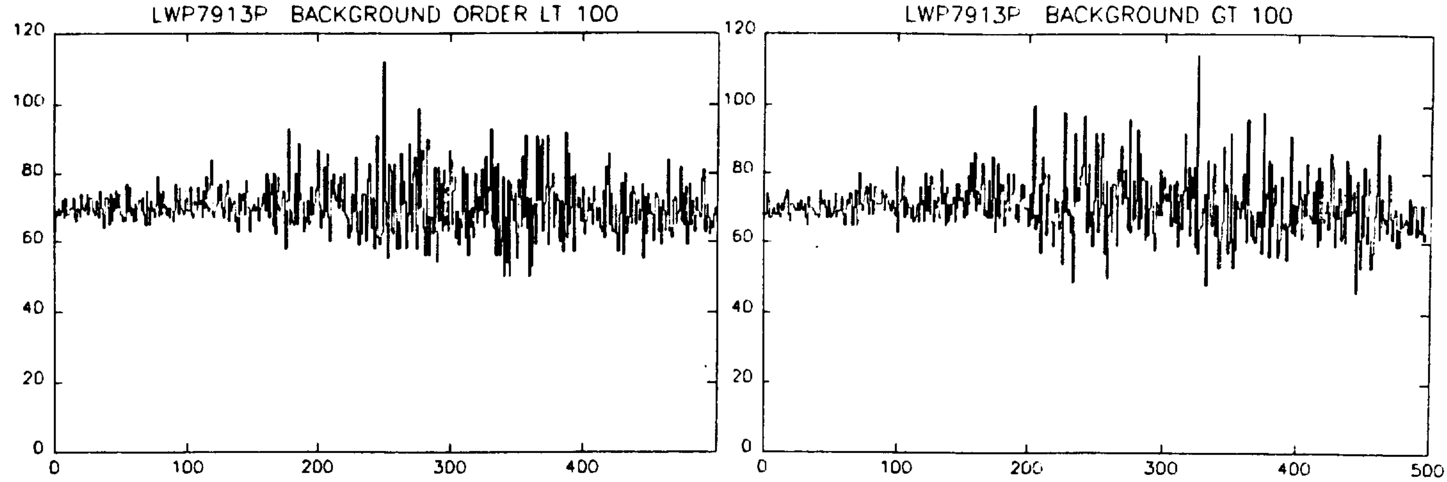

Figure 4: Unsmoothed interorder background scans on either side of order 100 in LWP 7913. These scans were extracted from the byte-scaled photometrically corrected image using the same algorithm as described in Figure 2 above. As in Figure 2, wavelength increases with increasing sample number. While the change in noise amplitude due to differences in camera focussing is apparent, the changing mean background level with wavelength seen in the IUESIPS extraction is not present.

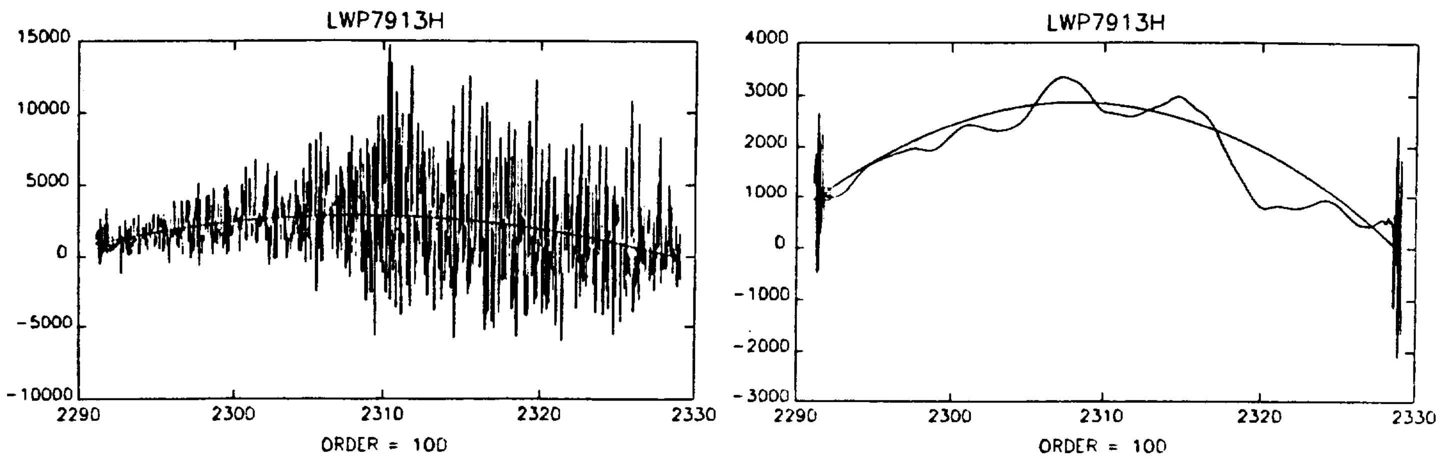

Figure 5a (left): Unsmoothed interorder background for LWP 7913. This version of the data was retrieved from the archive, and was processed using the old LWP ITF and old TCCAL. As a result, some of the point to point structure is different from the version showed in Figure 1. The smooth curve is a representation of the background derived by binning the interorder scan in 2 Å intervals, and then fitting a quadratic through the mean fluxes in each bandpass.

Figure 5b (right): Comparison of the IUESIPS filtered interorder background and the binned and fit background.

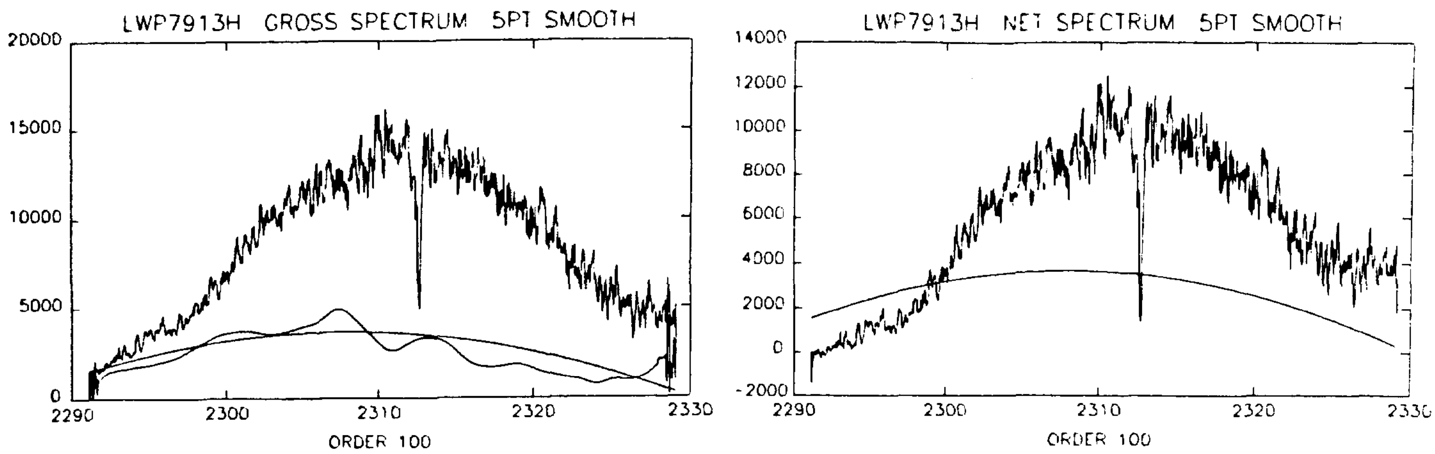

Figure 6a (left): Gross spectrum for LWP 7913 order 100 and IUESIPS and binned and fit backgrounds. This version of the data was processed using the new LWP ITF and old TCCAL.

Figure 6b (right): Net spectrum resulting from subtraction of the binned and fit background from the gross spectrum shown above. Note that the high frequency artifacts prominent in Figure 1b are eliminated.